Mechanically Biomimetic Gelatin–Gellan Gum Hydrogels for 3D Culture of Beating Human Cardiomyocytes

ACS APPLIED MATERIALS & INTERFACES

Research Article

Cite This: ACS Appl. Mater. Interfaces 2019, 11, 20589−20602

www.acsami.org

Mechanically Biomimetic Gelatin−Gellan Gum Hydrogels for 3D Culture of Beating Human Cardiomyocytes

Janne T. Koivisto,*[,†,‡] Christine Gering,[†] Jennika Karvinen,[†] Reeja Maria Cherian,[‡] Birhanu Belay,[§] Jari Hyttinen,[§] Katriina Aalto-Setälä,[‡,∥] Minna Kellomäki,[†] and Jenny Parraga*[,†]

[†]Biomaterials and Tissue Engineering Group, BioMediTech, Faculty of Medicine and Health Technology, Tampere University, 33720 Tampere, Finland

[‡]Heart Group, BioMediTech, Faculty of Medicine and Health Technology and [§]Computational Biophysics and Imaging Group, BioMediTech, Faculty of Medicine and Health Technology, Tampere University, 33520 Tampere, Finland

[∥]Heart Hospital, Tampere University Hospital, 33520 Tampere, Finland

Supporting Information

ABSTRACT: To promote the transition of cell cultures from 2D to 3D, hydrogels are needed to biomimic the extracellular matrix (ECM). One potential material for this purpose is gellan gum (GG), a biocompatible and mechanically tunable hydrogel. However, GG alone does not provide attachment sites for cells to thrive in 3D. One option for biofunctionalization is the introduction of gelatin, a derivative of the abundant ECM protein collagen. Unfortunately, gelatin lacks cross-linking moieties, making the production of self-standing hydrogels difficult under physiological conditions. Here, we explore the functionalization of GG with gelatin at biologically relevant concentrations using semiorthogonal, cytocompatible, and facile chemistry based on hydrazone reaction. These hydrogels exhibit mechanical behavior, especially elasticity, which resembles the cardiac tissue. The use of optical projection tomography for 3D cell microscopy demonstrates good cytocompatibility and elongation of human fibroblasts (WI-38). In addition, human-induced pluripotent stem cell-derived cardiomyocytes attach to the hydrogels and recover their spontaneous beating in 24 h culture. Beating is studied using in-house-built phase contrast video analysis software, and it is comparable with the beating of control cardiomyocytes under regular culture conditions. These hydrogels provide a promising platform to transition cardiac tissue engineering and disease modeling from 2D to 3D.

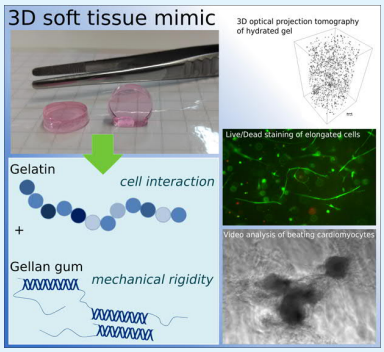

KEYWORDS: *hiPSC-derived cardiomyocytes, 3D hydrogel, gelatin, gellan gum, compression testing*

1. INTRODUCTION

The aim of tissue engineering (TE) is to create a new living tissue in vitro using a combination of biomaterial scaffolds, living tissue-specific cells, and biochemical factors.[1] In recent years, there has been a growing interest in the use of in vitro tissue and organoids as components for disease modeling, toxicology, and study of developmental biology.[2−5] In the case of cardiac disease modeling, human-induced pluripotent stem cell (hiPSC)-derived cardiomyocytes have been used to define the electrophysiological behavior of cardiomyocytes affected by specific genetic diseases.[5−8] As part of our earlier work, we reproduced the disease phenotype of genetic catecholaminergic polymorphic ventricular tachycardia in vitro and showed the proof of concept that iPSC-derived cardiomyocytes can reproduce a clinical drug response.[9] Furthermore, since cardiotoxicity is one of the most common causes of the drawbacks associated with many drugs, our group has been working on ways to improve methods for testing drug safety in 2D cardiac models.[10−12] To produce better biomimicking disease and cardiotoxicity models, however, a transition from 2D to 3D is needed to bridge the translational gap in drug discovery from single cell or 2D studies to clinical studies. A 3D disease model enables studying more intercellular interactions compared to 2D models, especially when comparing with single-cell studies.[3,13−15]

Till date, the most relevant cardiac 3D cell culture systems are engineered heart tissues, the so-called Biowire, 3D bioprinted structures, and even 3D printed organs-on-chip.[15−18] All of the above examples use an extracellular matrix (ECM) protein-based hydrogel scaffold, either Matrigel or gelatin methacrylate (GelMA), to support 3D cell culturing. In these studies, the focus is more on cardiomyocyte electrophysiology than on the relationship between the mechanical properties of the material and how cellular mechanotransduction affects the biological response.[19] Thus, more emphasis should be placed on the design and mechanical characterization of these soft biomaterial scaffolds.

Received: December 22, 2018
Accepted: May 17, 2019
Published: May 23, 2019

DOI: 10.1021/acsami.8b22343
ACS Appl. Mater. Interfaces 2019, 11, 20589−20602

To overcome the mechanical challenges of this specific biomedical application, new chemical cross-linking strategies for hydrogel production are needed. Noncovalent interactions have been used to produce hydrogels, mainly with electrostatic and hydrophobic interactions and hydrogen bonding. These hydrogels are usually relatively brittle with a narrow range of mechanical properties.[20,21] On the other hand, covalent cross-linking strategies have the ability to control the cross-linking density and, therefore, the mechanical properties. These strategies can result in higher elasticity, a key feature for the success of soft TE.

The cross-linking design should be chemoselective and efficient and should retain the biocompatibility of the polymer. In addition, gelation under physiological conditions could be beneficial for biomedical applications. Covalent hydrazone cross-linking is known to fulfil these requirements. Indeed, our previous studies have shown the elastic, biomimicking behavior of hydrogels obtained with this chemistry.[22−24]

In this work, we apply hydrazone chemistry to a combination of two well-known biopolymers in TE applications: gelatin and gellan gum (GG). Gelatin is a molecule derived from the abundant ECM protein collagen, and it is routinely used as a coating material in cardiac cell culture applications.[25,26] Gelatin hydrogel scaffolds can be formed by physical cross-linking, namely, thermal gelation. However, the gelation temperature is often below physiological requirements, and thus the use of these hydrogels in native form with cells is limited.[26] On the other hand, GG, a bacterial polysaccharide, is able to form hydrogels with tunable mechanical properties. The relatively bioinert nature of GG, however, does not support cell attachment.[21,27−29] Both GelMA and methacrylated GG (GGMA) have been photo-cross-linked into hydrogels and used to encapsulate cells.[26,30,31] They have even been combined in a double-network hydrogel with relatively good cytocompatibility.[32] However, the main limitations to using this approach for the fabrication of larger 3D tissues or organs is the phototoxicity of ultraviolet (UV) cross-linking and dependence on transparency of the hydrogel components.[33−35]

We have explored the use of these in situ cross-linkable hydrogels as biomimicking scaffolds for 3D cardiac disease modeling. In this study, we use 3D in-house-built microscopy to demonstrate the effects of hydrogel properties on cell morphology.[36] Our results show substantially more elongated fibroblast cells in 3D culture inside these hydrogels and clearly indicate better cytocompatibility than many other published cell results using the same hydrogel components.[32,37] On the basis of our findings, we used these hydrogels in a macroscale 3D culture of hiPSC-derived cardiomyocyte aggregates for the first time. The spontaneous beating behavior of the cardiomyocytes was analyzed with our previously developed motion tracking video analysis software.[11] Furthermore, we demonstrate that this rational hydrogel design supports the transition from 2D to 3D without interfering with the cardiomyocyte behavior and furthers the aim toward in vitro 3D hiPSC-derived cardiac disease modeling and drug screening.

2. EXPERIMENTAL SECTION

2.1. Materials. Gelatin A from porcine skin, GG (Gelzan CM Gelrite, M_w 1000 g mol^{-1}), spermidine trihydrochloride (SPD), sucrose, adipic dihydrazide (ADH), carbodihydrazide (CDH), dimethyl sulfoxide (DMSO), ethylene glycol, 1-ethyl-3-[3-(dimethylamino)-propyl]-carbodiimide (EDC), hydroxylamine hydrochloride, *N*-hydroxybentzotriazole (HOBt), 4-hydroxybenzaldehyde, deuterium oxide (99.9 atom % D, contains 0.05 wt % 3-(trimethylsilyl)-propionic-2,2,3,3-d4 acid, sodium salt), hydrochloric acid (HCl), sodium hydroxide (NaOH), sodium chloride (NaCl), and sodium periodate ($NaIO_4$) were purchased from Sigma-Aldrich (St. Louis, MO, USA). Dialysis membrane (Spectra/Por 12−14 kDa) was purchased from Spectrum Laboratories (Rancho Dominguez, CA, USA).

2.2. Preparation of ADH-Modified Gelatin (Gelatin-ADH). First, 300 mg of gelatin was dissolved in 100 mL of water, and 3.92 g (0.225 M) of ADH was added to this solution. The pH of the reaction mixture was adjusted to 6.8. Then, 576 mg (0.03 M) of EDC and 405 mg (0.03 M) of HOBt were dissolved in 3 mL of DMSO/water (1.5:1 v/v) and added to the reaction mixture drop by drop, while keeping the pH at 6.8 with 0.1 M NaOH and 0.1 M HCl during the mixture addition and for another 4 h. Then, the reaction was continued for another 20 h. The pH was adjusted to 7, and gelatin-ADH was exhaustively dialyzed against water for 2 d. Then, NaCl was added to produce a 7% (w/v) solution, and the product was precipitated in cold ethanol (4 vol equiv). Then, the product was dissolved in water and dialyzed against water for 2 days. Finally, the solution was lyophilized through a molecular weight cutoff 12−14 kDa dialysis membrane followed by freeze-drying.

2.3. Preparation of CDH-Modified Gelatin (Gelatin-CDH). First, 300 mg of gelatin was dissolved in 100 mL of water, and 3.6 g (0.4 M) of CDH was added to this solution. The pH of the reaction mixture was adjusted to 4.7 with 0.5 M HCl. Then, 575 mg (0.03 M) of EDC and 405 mg (0.03 M) of HOBt were dissolved in 3 mL of DMSO/water (1.5:1 v/v) and added to the reaction mixture drop by drop, while keeping the pH at 6.8 with 0.1 M NaOH and 0.1 M HCl during the mixture addition and for another 4 h. Then, the reaction was kept for another 20 h. Gelatin-CDH was exhaustively dialyzed against water for 2 days. Additional purification was carried out as described above followed by freeze-drying.

2.4. Preparation of Oxidized GG (GG-CHO). GG was modified by $NaIO_4$ oxidation according to the method previously reported by our group to produce GG-CHO at the modification degree of 25%.[22]

2.5. Polymer Characterization. To confirm the presence of hydrazide functionality, 20 mg of gelatin-ADH or gelatin-CDH was treated with 10 mL of 4-hydroxybenzaldehyde (20 mg mL^{-1}) in distilled water for 24 h at room temperature. The product was dialyzed and lyophilized as described above and analyzed by nuclear magnetic resonance (NMR) spectroscopy. All experiments were measured with a Jeol JNM-ECZR 500 MHz NMR spectrometer (Tokyo, Japan). The samples (5 mg) were dissolved in deuterium oxide (600 μL) containing an internal standard (0.05 wt % 3-(trimethylsilyl)-propionic-2,2,3,3-d4 acid, sodium salt). The samples were measured at 40 °C. The relative substitution was calculated by comparing the integral of the lysine amino acid peak at δ 3.0 ppm to the aromatic proton peak of 4-hydroxybenzaldehyde at δ 7.6 ppm. The presence of aldehyde groups in GG-CHO was qualitatively evaluated using Fourier transform infrared (FTIR) spectroscopy. FTIR-spectra from the GG-CHO polymer was measured on a PerkinElmer Spectrum One attenuated total reflection−FTIR spectrometer (Waltham, MA, USA) in the spectral range of 400−4000 cm^{-1}.

2.6. Hydrogel Preparation and Characterization. Modified gelatins and GG-CHO solutions were prepared separately by dissolving each polymer in an aqueous solution of 10% (w/w) sucrose or in Dulbecco's modified eagle medium (DMEM), as shown in Table 1. Before the hydrogel preparation, the gelatin polymer solutions were filtered using a Whatman FP 30/0.2 CA-S sterile filter (Thermo Fisher Scientific, MA, USA) at 37 °C, and the GG solutions were filtered using a Sterivex-GP 0.22 μm Millipore Express (polyethersulfone) sterile filter (Merck Millipore, MA, USA) at 60 °C. The solutions were kept at 37 °C, and then equal volumes (1:1) of the solutions were mixed for a few seconds by pipetting. The F7-SPD bioamine-GG compositions were prepared as stated previously[21]

DOI: 10.1021/acsami.8b22343
ACS Appl. Mater. Interfaces 2019, 11, 20589−20602

Table 1. Formulation of Hydrazone Cross-Linked Hydrogels Based on Gelatin and GG

formulation code	components	concentration [mg mL^{-1}]	gelation medium: 10% sucrose	gelation medium: DMEM/F-12 or PBS
F1-ADH	gelatin-ADH	40	+	
	GG-CHO	40		
F2-ADH	gelatin-ADH	40	+	
	GG-CHO	30		
F3-ADH	gelatin-ADH	40	+	
	GG-CHO	20		
F4-CDH	gelatin-CDH	60		+
	GG-CHO	60		
F5-CDH	gelatin-CDH	60		+
	GG-CHO	40		
F6-CDH	gelatin-CDH	40		+
	GG-CHO	40		
F7-SPD	unmodified GG	5	+	
	SPD	0.5	+	

with 1.5 wt % of SPD cross-linker per GG and used as the negative control.

2.7. In Vitro Hydrogel Degradation. For in vitro degradation tests, 500 μL of hydrogels were formed in Eppendorf tubes. A solution of 10 U mL^{-1} of collagenase II (Sigma-Aldrich, St. Louis, MO, USA) was added to the tubes, and aliquots were collected at the indicated time points and refreshed with fresh enzyme solution. The fluorescamine (Sigma-Aldrich, St. Louis, MO, USA) test was used to determine the presence of gelatin in the collected samples using a QuantaMaster PTI spectrofluorometer (Photon Technology International, Inc., Lawrenceville, NJ, USA) (excitation 390 nm, emission 465 nm).

2.8. Mechanical Characterization. Hydrogel samples were prepared in custom-made polydimethylsiloxane (PDMS) molds with a diameter of 12 mm and a height of 6 mm and tested at the earliest 2 h after gelation. PDMS was fabricated from the SYLGARD 184 base polymer and a curing agent (10:1, w/w, SYLGARD 184, Dow Corning, USA), acquired from Ellsworth Adhesives AB (Sweden). Mechanical testing was performed, as we have previously described in detail, using a BOSE ElectroForce BioDynamic 5100 machine equipped with a 225 N load sensor and Wintest 4.1 software (Bose Corporation, Eden Prairie, MN, USA).[21] Unconfined compression was performed with a constant 10 mm min^{-1} strain rate until 75% strain of the original height was reached. The fracture point was seen as a clear drop in the stress−strain curve.

To obtain a relevant reference for our hydrogel's biomimicry of the tissue, we used the compression testing data from fresh heart tissues of New Zealand white rabbits, based on our previous results.[22] The compression samples were cut from both the left and right heart ventricle, compressed in the direction perpendicular to the beating direction, and pooled together. The rabbit tissues were obtained from animal experiments conducted at the Tampere University Medical School.

Statistical analysis of the mechanical testing data was performed by SPSS Version 25.0 (IBM SPSS Statistics for Windows, NY, USA). The data were presented as mean ± standard deviation. One-way analysis of variance was performed with a confidence level of 95%. P values less than 0.05 were considered as statistically significant. Pair comparisons of data were done with the Tukey post-hoc test to identify significant differences between the hydrogel formulations.

2.9. Fibroblast Hydrogel Cell Culture. The commercial human lung fibroblasts (WI-38, Culture Collections, Public Health England, United Kingdom) were cultured and expanded in Nunc T75 culture flasks (Thermo Fisher Scientific, USA) with DMEM/Ham's Nutrient Mixture F-12 (F-12 1:1; Thermo Fisher Scientific, USA) supplemented with 10% fetal bovine serum (FBS; South American Origin, Biosera, Finland) and 50 U mL^{-1} penicillin/streptomycin (Pen/Strep; Thermo Fisher Scientific, USA). For cytocompatibility testing, fibroblasts were detached from the culture flask via trypsin (Lonza, Basel, Switzerland) treatment and then counted and plated with 30 000 cells cm^{-2} under 2D conditions and with 300 000 cells mL^{-1} under 3D conditions. To test the cytocompatibility of the modified gelatin, separate cell culture wells were dip-coated with gelatin-ADH or gelatin-CDH (40 mg mL^{-1}) with 1 h incubation at 37 °C.

Hydrogel cell cultures were conducted both on top of the hydrogel (2D) and encapsulated inside the hydrogel (3D), with all hydrogel compositions listed in Table 1. In the 2D experiment, the hydrogel was cast in the well plate 20 min before the cells were plated on top. In the 3D experiment, 30 μL of cell suspension was mixed with gelatin-ADH or gelatin-CDH and GG-CHO simultaneously during gelation to form a total of 330 μL of hydrogel. Cell culture medium was applied on top of the samples after ∼20 min of gelation time. Unmodified gelatin coating was used as a control in all cell experiments. All coating and hydrogel cell tests were done on a Greiner CELLSTAR 48-multiwell plate (Sigma-Aldrich).

After 3 and 7 days of culturing, the samples were stained with a Live/Dead (Thermo Fisher Scientific, USA) cell viability kit. The fluorescent calcein-AM (at 0.2 μM) stains intact cells green, and ethidium homodimer-1 (at 1.0 μM) stains dead cells red. After 1 h of incubation at room temperature with a rocker, the cells were imaged with an Olympus IX51 inverted microscope and an Olympus DP30BW digital camera (Olympus, Finland). Staining concentrations were double that recommended by the kit instructions to allow for faster diffusion under 3D hydrogel conditions. During wide-field microscopy, the 3D position in the middle of the hydrogel was verified by using the 2D cell control at the well-plate bottom as a reference point and changing the focus distance accordingly.

The cell numbers were quantified using ImageJ (Version 1.39, US National Institutes of Health, Bethesda, MD, USA)[38] particle counting algorithm based on at least three parallel Live/Dead stained images taken with 4× magnification from all studied conditions. Fibroblast viability percentage was calculated from the detected live and dead cell area according to the following equation

$$\text{Viability } \% = \frac{\text{area of live cells}}{\text{area of live cells} + \text{area of dead cells}} = \frac{\sum_{i=1}^{n} L_i}{\sum_{i=1}^{n} D_i + L_i}$$

2.10. Optical Projection Tomography Imaging. An in-house built optical projection tomography (OPT) system in transmission mode was used for imaging cells encapsulated in the hydrogel to visualize the 3D morphology of fibroblasts under selected hydrogel conditions.[36,39] Cell cultures were prepared in fluorinated ethylene propylene tubes with water matching the refractive index and submerged inside a cuvette filled with water for imaging. All OPT samples were imaged after 7 days of culture. A white light-emitting diode source (Edmund, USA) was used to illuminate the sample. The transmitted light was detected by a 5× infinity-corrected objective (Edmund, USA) with a numerical aperture of 0.14 and imaged with a sCMOS camera (ORCA-Flash 4.0, Hamamatsu, Japan). The sample was rotated 360° while a total of 400 projection images were captured at 0.9° intervals. 3D reconstruction was computed in MATLAB from projection images using standard filtered back-projection algorithm.[36] Visualization in 3D was done in Avizo software (Thermo Fisher Scientific, Waltham, MA, USA).

2.11. Cardiomyocyte Differentiation. The Ethics Committee of Pirkanmaa Hospital District gave approval to conduct research on hiPSC lines (Aalto-Setälä R08070). The hiPSC line UTA.04602.WT was cultured and characterized at the stem cell state, as previously described.[40] The cardiomyocyte differentiation was done by modulating Wnt signaling with small molecules, according to the protocol published by Lian et al. 2012.[41] In short, differentiation was initiated by plating 700 000 hiPSCs/well in a Nunc 12-multiwell plate (Thermo Fisher Scientific, USA) in feeder-free condition on Geltrex-

DOI: 10.1021/acsami.8b22343
ACS Appl. Mater. Interfaces 2019, 11, 20589−20602

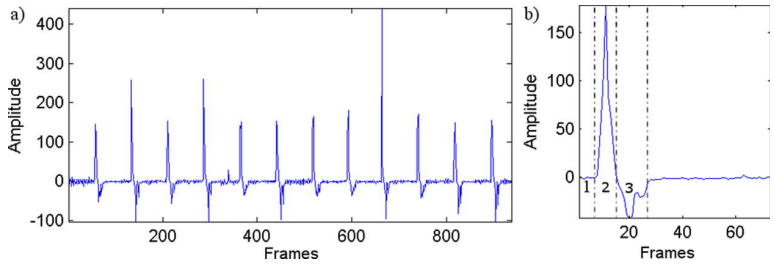

Figure 1. Beating pattern of cardiomyocyte aggregate in F4-CDH hydrogel as an example of the BeatView analysis. This is the same aggregate as in Video S8. Graph (a) shows regular beating rhythm; (b) shows the breakdown of a single beat into relaxed state (1) and contracting (2) and relaxing (3) movements.

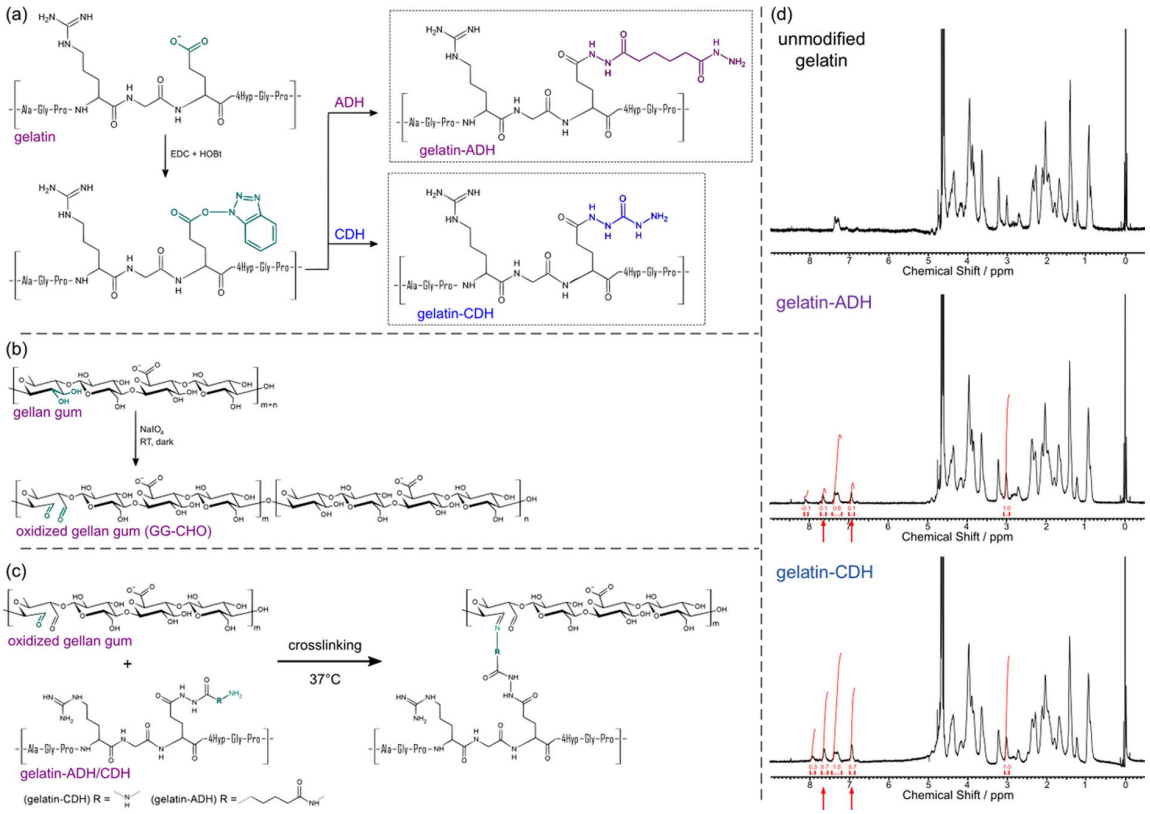

Figure 2. (a) Chemical modification of gelatin carboxylic groups with hydrazide molecules ADH (provides 10-atom bridge) and CDH (provides 5-atom bridge). (b) Periodate oxidation of vicinal diols in GG. (c) Hydrazone cross-linking reaction between gelatin-ADH/CDH and GG-CHO. (d) ^{1}H NMR-spectra of nonmodified gelatin, gelatin-ADH, and gelatin-CDH modifications. The arrows highlight the appearance of aromatic protons in gelatin-ADH and gelatin-CDH spectra after the coupling reaction of CDH and ADH with 4-hydroxybelzandehyde. Chemical modification was successful based on the appearance of extra peaks.

coating (Thermo Fisher Scientific, USA) in mTeSR1 medium (STEMCELL Technologies, Canada) supplemented with 50 U mL^{-1} Pen/Strep for 4 days. Ten days after initiation, the medium was changed to RPMI (Thermo Fisher Scientific, USA) supplemented with B27(−insulin) (Thermo Fisher Scientific, USA) and 50 U mL^{-1} Pen/Strep. During this time, on day one, 8 μM CHIR99021 (REPROCELL, United Kingdom) was applied to the cells. After 24 h, CHIR99021 was removed. On day3, 5 μM IWP-4 (R&D Bio-Techne, USA) was added for 48 h. From day 10 onwards, B27(−insulin) was changed to B27(+insulin) (Thermo Fisher Scientific, USA), and the cells were cultured in this medium until they were used for the hydrogel experiments.

2.12. Cardiomyocyte Hydrogel Cell Culture. After differentiation, beating cardiomyocyte areas were cut with a scalpel under a microscope and collected. Then, the aggregates were partially dissociated to loosen the cell-to-cell bonds inside the aggregate and to better allow the attachment on the hydrogel. Dissociation was modified from the study of Ahola et al. 2014.[11] The enzymatic dissociation buffers were applied to the cells incubated at 37 °C: First buffer for 45 min, second buffer for 15 min, and third buffer for 10 min, but no mechanical dissociation was done. The gentle dissociation treatment loosens the cardiomyocyte aggregate and makes it more susceptible to attach on to the hydrogel surface. Four aggregates were plated per well with all coating and hydrogel preparations (2D and 3D), as described above for fibroblasts. Cells were cultured with KnockOut-DMEM medium (Thermo Fisher Scientific, USA) supplemented with 20% FBS, 1% nonessential amino acids (Cambrex, NJ, USA), 2 mM GlutaMAX (Thermo Fisher Scientific, USA), and 50 U mL^{-1} Pen/Strep. The medium was changed every 3 days, always 1 day before analysis, and the cells were cultured for 7 days maximum.

DOI: 10.1021/acsami.8b22343
ACS Appl. Mater. Interfaces 2019, 11, 20589−20602

2.13. Analysis of Cardiomyocyte Hydrogel Cell Culture. The cardiomyocyte cultures were primarily analyzed by phase contrast microscopy using a Nikon Eclipse TS100 (Nikon Corporation, Japan) microscope with a Nikon accessory heating plate, and monochrome 8-bit videos were acquired with an Optika DIGI-12 (Optika Microscopes, Italy) camera. The video recording of beating cardiomyocytes was done with the same setup using 60 frames per second, recording for 30 s. The beating is temperature sensitive, and our measurement setup has been previously verified to be at 37 °C inside the well plate.[42] The videos were analyzed with BeatView software.[11] Figure 1 shows a representative beating pattern of a cardiomyocyte aggregate.

Additionally, the cardiac nature of the differentiated cardiomyocytes was verified using real time polymerase chain reaction (RT-PCR), qPCR, and immunocytochemical staining. For PCR, the total RNA from the cardiomyocyte aggregates in the hydrogel was isolated using the Qiagen RNeasy kit (Qiagen, Germany) after 2 weeks in culture. For the RNA extraction, the culture medium was removed, and the hydrogel was washed in phosphate-buffered saline (PBS) briefly three times. The cardiomyocyte aggregates in the hydrogel were cut with a scalpel under a microscope and collected in a microcentrifuge tube. The hydrogel surrounding the cluster was partially digested by adding 100 μL of pronase solution (stock 10 mg mL^{-1} in water, Sigma-Aldrich, St. Louis, MO, USA) and incubated at 37 °C for 5 min with mild shaking. The digested hydrogel solution was then added directly to the RNeasy lysis buffer and homogenized, and RNA was extracted according to the manufacturer's instructions. DNase I-treated total RNA was reverse-transcribed using a high capacity cDNA reverse transcription kit (Applied Biosystems, Foster City, CA, USA). The cDNA was amplified by the TaqMan Universal Master Mix (Applied Biosystems) using the BioRad CFX384 real-time PCR detection system. Samples were analyzed in triplicates, and glyceraldehyde 3-phosphate dehydrogenase (GAPDH) was used for normalization of expression levels of individual genes, which was calculated by the $\Delta\Delta C_T$ method.[43] TaqMan assays used in the qPCR protocol are presented in Table S1.

Immunocytochemical staining was done with the previously reported, optimized protocol for 3D cell culture.[21] In brief, cultures were fixed with 4% paraformaldehyde for 30 min. After a brief wash in PBS, nonspecific staining was blocked with 10% normal donkey serum (NDS), 0.1% Triton X-100, and 1% bovine serum albumin (BSA) (all from Sigma-Aldrich, St. Louis, MO, USA) in PBS for 1 h in room temperature, followed by another wash in 1% NDS, 0.1% Triton X-100, and 1% BSA in PBS. Then, a combination of primary antibodies, troponin T (1:1750) from goat and α-actinin (1:1250) from mouse, dissolved in 1% NDS, 0.1% Triton X-100, and 1% BSA in PBS, was applied to the cells and incubated at 4 °C for 2 days. The samples were washed three times in 1% BSA in PBS (first 5 min, followed by 2 × 1 h) and then incubated for 2 days at 4 °C with Alexa Fluor 488 conjugated to donkey anti-mouse (1:800) and Alexa Fluor 568 conjugated to donkey anti-goat (1:800) in 1% BSA in PBS. The samples were washed three times (first 5 min, followed by 2 × 1 h) in PBS. As the last step, 4′,6-diamidino-2-phenylindole (DAPI) for nuclei staining was applied at 1:2000 concentration in 1% PBS, and the samples were stored light-protected at 4 °C. The cells were imaged with an Olympus IX51 inverted microscope and an Olympus DP30BW digital camera (Olympus, Finland) similar to Live/Dead stained fibroblasts.

3. RESULTS AND DISCUSSION

3.1. Modification of Biopolymers. To form hydrazone cross-links between GG and gelatin, we hypothesized that hydrazide groups could be introduced to the gelatin backbone to form cross-links with the aldehyde groups generated in the GG molecule (Figure 2). Our results show that the carboxylic group present in the gelatin molecule can be modified with ADH or CDH, and the modifications were confirmed by ^{1}H NMR spectroscopy (Figure 2). The spectra of gelatin-ADH and gelatin-CDH after the derivatization with 4-hydroxybenzaldehyde shows the appearance of protons at δ 6.9 ppm and δ 7.6 ppm, compared with unmodified gelatin, and indicates the presence of hydrazide groups available for the cross-linking process. The integrated intensity of these protons was much higher for gelatin-CDH (0.7) than for gelatin-ADH (0.1). In addition, the peak at δ 7.3 ppm, corresponding to phenylalanine amino acid, increased in gelatin-CDH (1.0) compared with gelatin-ADH (0.6) because of the contribution of the aromatic group in 4-hydroxybenzaldehyde. As a reference, we used the amino acid lysine with a signal at δ 3.0 ppm. The degree of modification of gelatin-CDH was slightly higher than that of gelatin-ADH. This was likely due to the formation of bonds between two molecules of gelatin generating an adduct.[44] On the other hand, GG was modified through periodate oxidation (GG-CHO), and the presence of aldehyde groups was corroborated by FTIR, where a typical aldehyde shoulder was detected at 1733 cm^{-1}, as shown in Figure S1.[22]

3.2. Gelatin-GG Hydrogel Preparation. Hydrazide-modified gelatins and oxidized GG (GG-CHO) form hydrazone bonds that are capable of creating a hydrogel under physiological conditions without any external energy, cross-linkers, or catalysis. To obtain self-standing hydrogels with adequate mechanical properties, several volume ratios and polymer concentrations were tested. The detailed hydrogel formulations obtained and studied in this work are described in Table 1 in the Experimental Section. Briefly, formulations of F1−F3-ADH are composed of gelatin-ADH and GG-CHO, and formulations of F4−F6-CDH are composed of gelatin-CDH and GG-CHO. In general, poor gelation was shown by concentrations below 20 mg mL^{-1} (2%) of gelatin-ADH and 30 mg mL^{-1} (3%) gelatin-CDH. Forming the gels with components of equal concentration, the volume ratio 1:1 yielded the best gelation. When the ratio was changed by increasing the volume of the gelatin component, the gels became very weak. The maximum amount of gelatin required to produce a true hydrogel was 60% w/w in polymer weight, which was achieved with gelatin-CDH because of the higher modification degree compared with gelatin-ADH. The gelatin-ADH or gelatin-CDH with GG-CHO components form a sticky and true gel within seconds. Complete gelation is reached within 5 min for F1−F3-ADH and within 10 min for F4−F6-CDH.

Cross-linking of GG with calcium ions and PBS or DMEM to make covalently cross-linked hydrogels that are mechanically robust has been extensively explored.[27] However, these cross-linking methods lack cytocompatibility. Here, with the inclusion of gelatin, it is expected that the cell interaction with the material will improve significantly because of the natural cell adhesion motifs (e.g., RGD) and the matrix metalloproteinase-mediated degradability present in gelatin.[45] The simplicity of this cross-linking method provides the opportunity to control the mechanical properties, for example, by adjusting the ratio or concentration of the polymers in the system.

Our approach simplifies hydrogel formation relative to other gelatin cross-linking schemes because it does not require high ion concentrations, varying temperature during gelation, or UV light and enables gelation under mild, physiological conditions.[31,46,47] In general, we can state that our hydrogel production method using simple casting is an easier and biologically safer way to produce 3D culture substrates for cardiomyocytes than many of the other published methods.

DOI: 10.1021/acsami.8b22343
ACS Appl. Mater. Interfaces 2019, 11, 20589−20602

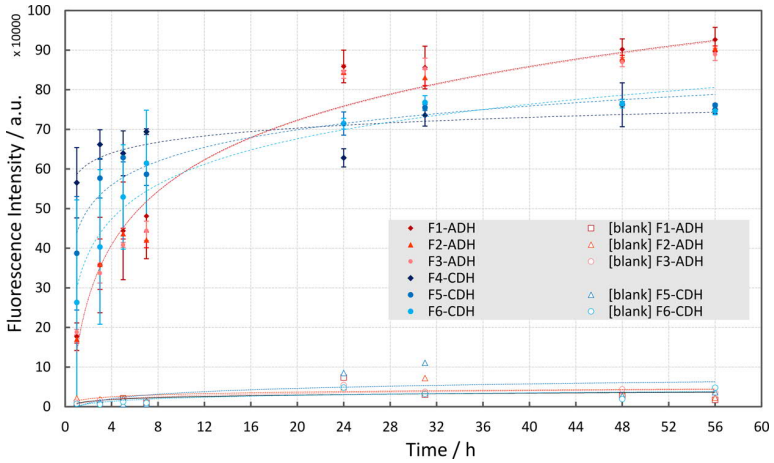

Figure 3. Degradation profiles of the tested hydrogels incubated with collagenase for 56 h. Values represent the mean and standard deviation. Sigmoidal curve fits were applied to the data.

For example, even though the layer-by-layer technique described by Amano et al. 2016 produces well-controlled 3D structures, it requires longer fabrication times per sample.[48] Moreover, the Biowire method by Nunes et al. 2013 requires a special, custom-made mold to retain the weak hydrogel until the cells produce their own ECM, and even more complex molds are required for the microphysiological system reported by Mathur et al. 2015.[16,49] In contrast, our self-supporting hydrogel can be cast, or even injected, in many different shapes for 3D cell encapsulation. Moreover, it could replace the Matrigel or GelMA used in the aforementioned 3D cardiomyocyte culture systems.[16,48,49] For future cardiac drug-screening studies, however, a high throughput study setup suitable for our gelatin-GG hydrogel would be cell-encapsulating droplets that can be studied optically and electrophysiologically, as suggested by Oliveira et al. 2016.[50]

3.3. In Vitro Hydrogel Degradation. To evaluate the degradation profile, the hydrogels were incubated at 37 °C in collagenase (10 U mL^{-1}) solution for 56 h, and sample aliquots were periodically taken. The presence of gelatin was evaluated by fluorescence. Figure 3 shows the degradation profiles of the hydrogels. The concentrations used for the ADH or CDH formulations did not show any significant differences within either chemistry type, but the degradation rate of CDH hydrogels showed a clear difference when compared with ADH hydrogels. As expected, the degradation rate decreased with F4−F6-CDH hydrogels, whereas the different degradation observed between the hydrogels based on CDH or ADH may be attributed to an increased number of cross-links (covalent and ionic) in F4−F6-CDH. Compared with the previously developed gelatin-based hydrogels exposed to similar concentrations of collagenase, our CDH gelatin-based hydrogels showed better resistant to collagenase, albeit they have been shown to be less resistant than GelMA-based hydrogels.[51,52] This lack of resistance is due to the higher cross-linking density of GelMA, which is not always beneficial for nutrient diffusion and cell spreading.

3.4. Mechanical Properties of Hydrogels. Mechanical characterization of these hydrogels was carried out as uniaxial compression testing at a compression rate of 10 mm min^{-1} under ambient conditions. The sticky characteristic of the specimens meant that they had to be cut out from their PDMS molds, and their difficult handling likely decreased the repeatability of some of the specimens.

As fresh, healthy human heart tissue is not easily available for mechanical testing, many different mammalian tissues have been used in the literature for the determination of the mechanical properties of the tissue, and we chose to use rabbit heart as the reference as it was readily available.[53−55] Figure 4 shows the representative stress−strain curves of the measured gelatin-GG hydrogel compositions and compares them with the fresh rabbit heart muscle.[22] All samples were initially very easily deformed, but the strain-hardening behavior of gelatin-CDH-based hydrogels and rabbit heart is remarkably similar and occurs at the same strain values of over 40%. The gelatin-ADH-based hydrogel's strain hardening effect is smaller and occurs at even higher strains than with gelatin-CDH-based hydrogels. Because the chemical modification does not affect the groups available for ionotropic cross-linking in GG, extra cross-linking was expected to occur in gelatin-CDH-based hydrogels as they were produced in DMEM/F-12.

The gelatin-ADH-based hydrogels had a fracture strength of 23 to 27 kPa, whereas F6-CDH had a fracture strength of 97 kPa and F5-CDH of even over 300 kPa, as can be seen in Figure 4. All tested compositions exhibited fracture between 60 and 75% strains, indicating high elasticity. For both modifications, the highest strength hydrogel was the composition with an uneven amount of gelatin to GG-CHO (F2-ADH and F5-CDH). This indicates that not all cross-linking points are used in compositions with even concentrations of both components; thus additional cross-linking occurs with the increase of hydrazide groups. Meanwhile, the increase in GG-CHO enhances the stability of the hydrogels but also makes the hydrogels slightly more brittle.

In the literature, the mechanical properties of hydrogels are too often intermixed, and the exact same parameters are not compared. For example, in the case of viscoelastic materials, different compression rates affect the material response, and in consequence, elastic regions are being defined differently.[20,56] Thus, we only compared our results with previous results from unconfined compression at 10 mm min^{-1} strain rate. When comparing the current gelatin-GG hydrogels with our previously published bioamine-GG, hyaluronic acid-GG hydrazone, and plain hyaluronic acid hydrazone hydrogels, the gelatin-ADH-based hydrogels more closely resemble the

DOI: 10.1021/acsami.8b22343
ACS Appl. Mater. Interfaces 2019, 11, 20589−20602

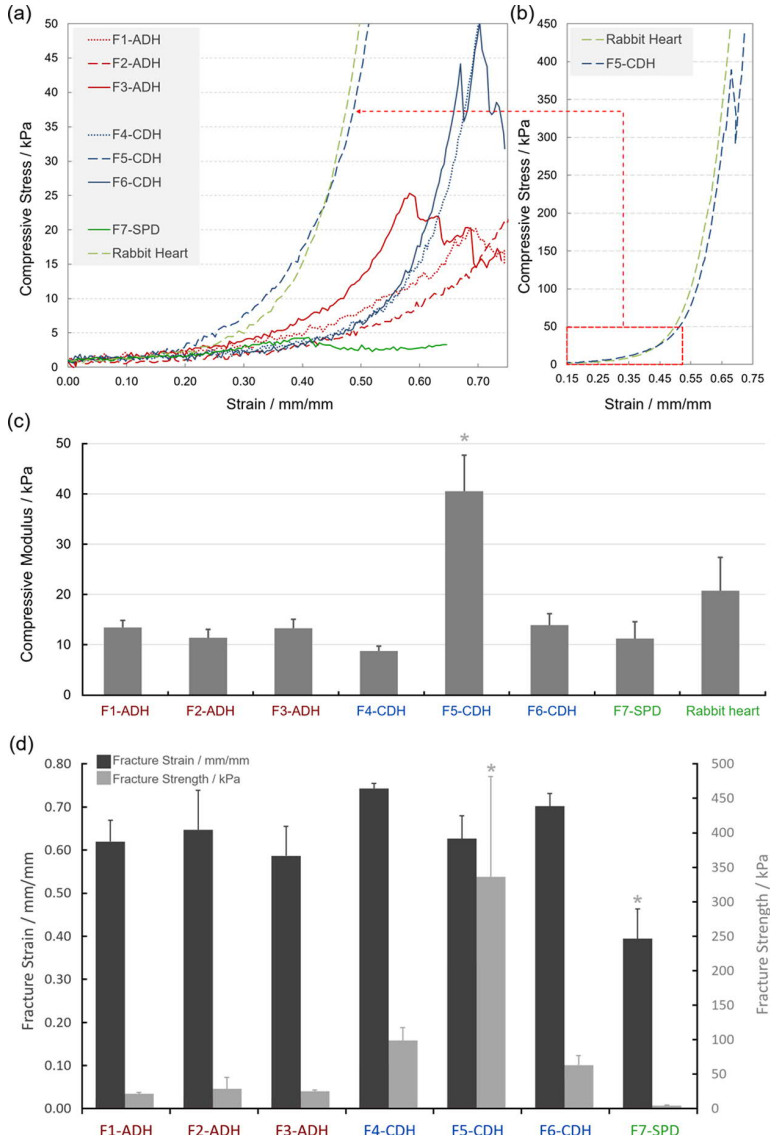

Figure 4. Representative stress−strain curves of the different hydrogel compositions and the rabbit heart tissue. (a) All representative curves with stress range 0 to 40 kPa. (b) Extended graph with the stress scale up to 450 kPa to highlight the similarities between F5-CDH and rabbit heart tissue. (c) Compressive moduli of the hydrogels compared to the rabbit heart. (d) Fracture strain and strength measured by compression testing. The *y*-axis on the left and the dark gray bars show the fracture strain relative to the original sample height. The *y*-axis on the right and the light gray bars show the fracture strength. In (c) and (d), $n = 5$; * = significantly different from other formulations at $p < 0.05$.

hyaluronic acid-based hydrogels.[21−23] The bioamine-GG, such as F7-SPD, is rather brittle in comparison to any hydrazone cross-linked hydrogels, with fracture occurring already at 35% strain. The cross-linking chemistry in all of these materials is the same and consistently produces similar mechanical behavior. This shows that the exact biopolymer concentration has only a minor effect on the mechanical behavior, whereas the chemistry used (ADH or CDH) determines the mechanical properties. At the same polymer concentration, F6-CDH is stronger than F3-ADH. However, F5-CDH has more than a 10-fold increase in fracture strength and a 2-fold increase in compressive modulus, compared to other CDH formulations, and thus substantially higher strain-hardening behavior while still being very elastic and compliant until 40% strain.

One clear effect of changing to hydrazone cross-linking from our previous ionotropic bioamine cross-linking of GG was the change in the compression behavior from being rather brittle to highly elastic. This change in compression behavior was accompanied by an increase in the fracture strength.[21] In cardiac TE, the mechanical properties of the growth substrate affect the spontaneous beating of cardiomyocytes.[57,58] In the case of a very rigid polystyrene substrate, the standard 2D well plate, the upper part of the cell is free to move, allowing for the unconstrained beating of the cell.[11] For 3D matrices, however, the cell is in contact with the surrounding scaffold material in all directions. As a result, the constant spontaneous beating of the cell while encapsulated could be prevented, if the hydrogel is not elastic and compliant enough, whereas a biomimicking hydrogel could support cell differentiation and further maturation.[57,58]

DOI: 10.1021/acsami.8b22343
ACS Appl. Mater. Interfaces 2019, 11, 20589−20602

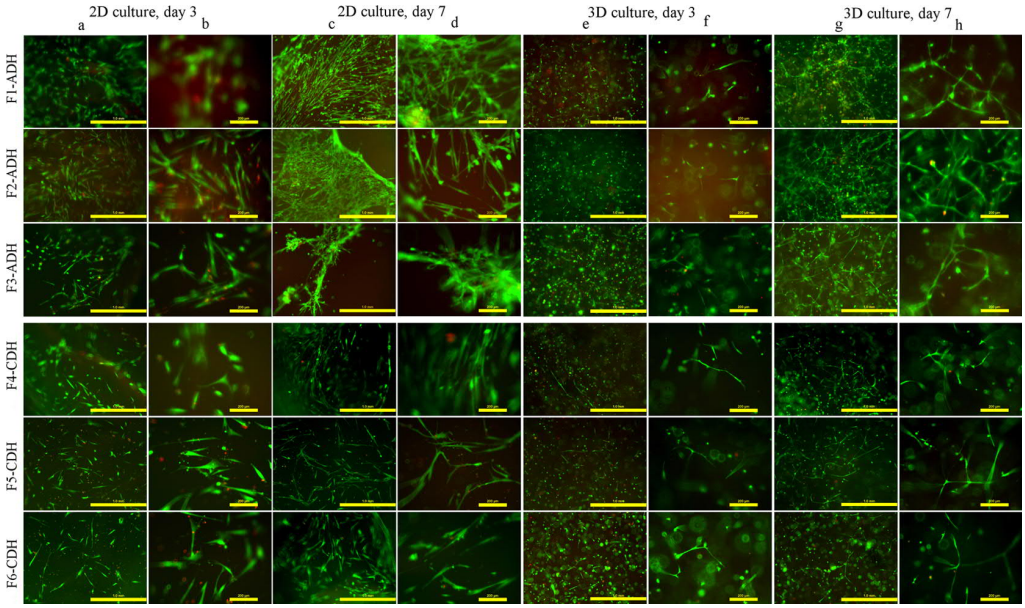

Figure 5. Representative images of Live/Dead stained fibroblast cell cultures in all tested hydrogel formulations and both 2D and 3D culture conditions at the 3-day and 7-day time points. The 3D cultures were imaged in the middle of the hydrogel. Green indicates live cells and red indicates dead cells. Rows (a), (c), (e), and (g) are with lower magnification, and the scale bar length is 1000 μm; rows (b), (d), (f), and (h) are with higher magnification with a scale bar length of 200 μm.

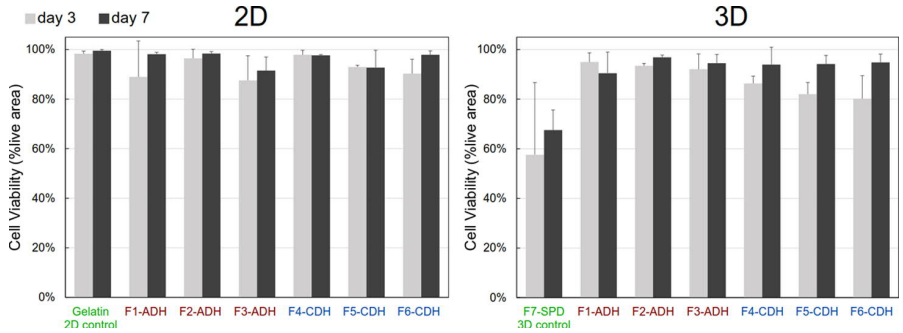

Figure 6. Measured fibroblast viability percentage based on amount of live cells compared to amount of all cells, 4× magnification images. Error bars represent mean values ± standard deviation, $n \geq 3$.

One of the earliest reports about increasing hydrogel strength by blending GG with gelatin is from US patent 4 517 216.[46] However, the patent is aimed at food applications and requires heating the components to 80 °C, which clearly exceeds the range suitable for cell encapsulation applications.[46] More suitable gelatin-GG hydrogels for cell encapsulation have been presented by Shin et al. 2012 and Melchels et al. 2014, both using GelMA that requires UV cross-linking. Both groups show a significant increase in the hydrogel fracture strength by the addition of GG to GelMA.[32,59] Shin et al. also describe a similar elasticity and strain hardening effect as shown for our hydrogels in Figure 4.[32] When compressed alone, GelMA has higher fracture strength and strain than our strongest hydrogels, whereas GGMA alone is clearly more brittle and has lower fracture strength than our hydrogels.[31,32,37,60] By combining GelMA and GGMA into a double-network GelMA-GGMA hydrogel with double the polymer concentration of ours, the fracture strength and strain are increased even further.[32] Wen et al. 2014 present another double-network hydrogel composed of GG and gelatin that utilizes enzymatic cross-linking instead of UV.[61] They report tensile, but not compressive, mechanical test results, and the measured values of fracture strength and strain are in the same range as ours, if tested without the initiation of a double network by Ca^{2+} addition. With the double network, their highest concentrations produced higher strength and elasticity than ours.[61]

3.5. Cell Culture Studies. *3.5.1. Hydrazide-Modified Gelatin Cytocompatibility.* First, native and modified gelatins (gelatin-ADH and gelatin-CDH) were used as coating at 40 mg mL^{-1} for seeding human lung fibroblast WI-38 cells to test the cytocompatibility. The WI-38 cell line was chosen for this purpose based on ISO 10993-5:2009 standard (Biological Evaluation of Medical Devices. Part 5: Tests for In Vitro Cytotoxicity) as a well-known, general purpose human cell line for initial biomaterial screening.[62] The results showed that the modifications did not alter the gelatin's inherent ability for cell attachment and proliferation. The cells attached and showed an elongated morphology after overnight culture under all gelatin-coating conditions (data not shown). In a prolonged culture, the cells became confluent in a week (Figure S2).

3.5.2. Hydrogel Cell Culture of Fibroblasts. After successful cytocompatibility tests with gelatin modifications, the fibro-

DOI: 10.1021/acsami.8b22343
ACS Appl. Mater. Interfaces 2019, 11, 20589−20602

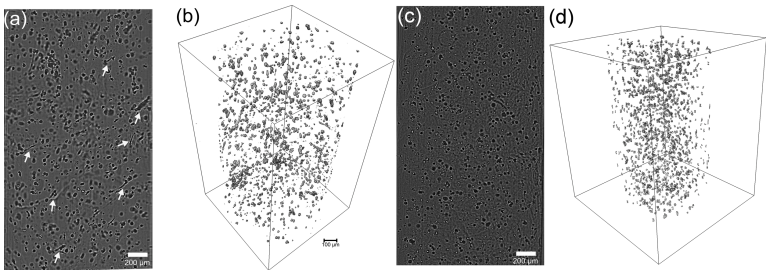

Figure 7. Bright-field OPT visualization of fibroblast cell culture under 3D hydrogel condition. (a) Single projection image of F3-ADH hydrogel, with highly elongated cells highlighted with arrows, (b) 3D reconstruction of the previous giving a view of the whole sample, (c) single projection image of negative control F7-SPD hydrogel, and (d) 3D reconstruction of the previous.

blasts were cultured on top of the hydrazone cross-linked hydrogels listed in Table 1 to study cell attachment and elongation. The fibroblasts were also encapsulated in the same hydrogels to study the cytocompatibility of the cross-linking reaction as well as viability and elongation under 3D conditions. Since gelatin has integrin binding sites and enzymatic cleavage sites, we hypothesized that the cells encapsulated in the hydrogels would be able to elongate in 3D. The initial cell response was examined after 3 days of culture and prolonged culture on day 7. Live/Dead staining was used to visually assess the viability and morphology of the fibroblasts, as shown in Figures 5 and 6. The negative control F7-SPD is shown in Figure S2. On day 3, the cells were already highly elongated and even more so at day 7.

As can be seen in Figure 5, the fibroblast cells are predominantly alive under all tested conditions and at both time points (day 3 and day 7). First, this indicates that the chemical modification is not harmful to the cells and that the cross-linking reaction is efficient and does not leave too many unreacted aldehyde groups to affect cell viability after gelation. A few dead cells were present on day 3, but the number of live cells was much higher, as seen from the viability in Figure 6 being between 80 and 95% for all hydrazone cross-linked hydrogels. Although the initial cell numbers were the same, the cultures seemed more confluent on day 7, indicating cell proliferation. Second, the cells exhibited a high degree of elongation in all directions in 3D under all tested conditions. However, a normal widefield microscope does not convey the status of the cells in a large hydrogel sample but rather gives a snapshot of the culture at a certain position. A holistic view of the sample is critical when evaluating the quality of tissue development.[63] Therefore, we use OPT to visualize several cellular features in a label-free 3D system.[39] Here, we emphasized morphology and elongation as parameters of cytocompatibility (Figure 7 and Videos S1 and S2). Moreover, both the shape and distribution of the cells throughout the hydrogel can be viewed from various angles as shown in Video S1. As can be seen with the F3-ADH hydrogel, a good proportion of the cells are elongated and uniformly distributed in 3D, indicating hydrogel homogeneity in composition and good diffusion of nutrient throughout.

As the cell morphology was well visible in the Live/Dead images, an additional phalloidin or immunocytochemical cytoskeleton staining was deemed unnecessary. The F4-6-CDH hydrogels seemed to have more elongated cells at the earlier time point, and even longer spindlelike cells were seen at the later time point compared with the F1-3-ADH hydrogels. This highly elongated cell morphology is typical for these WI-38 fibroblasts under 2D culture conditions on cell culture plastic.[64] Under 3D culture conditions and in normal cytocompatibility testing, this high degree of elongation is rarely seen. In fact, none of the gelatin-GG studies discussed in Section 2.4 report similar elongation as observed here.[32,59,61] Elongation has been previously reported with mouse fibroblasts in the click-chemistry cross-linkable gelatin hydrogel,[51] and moderate polarization of human adipose stem cells has been reported in the GG-based hydrogel, if collagen is added.[50] Qualitatively estimating the amount of elongation shown in Figure 5 is magnitudes higher compared with either of those studies.[50,51] The elongation of human fibroblast cells on top of a GG microsphere surface modified with gelatin has been previously reported by Wang et al. 2008.[65] However, they did not encapsulate the cells inside the gel microspheres because of the complexity of the cross-linking process. In summary, we have achieved a higher degree of elongation and viability of human fibroblast cells in the encapsulated condition than has been previously reported. Thus, our GELA-GG hydrogel presents an exciting step toward 3D tissue development.

3.5.3. Hydrogel Cell Culture of Cardiomyocytes. Encouraged by the fibroblast results, we studied hiPSC-derived cardiomyocyte aggregates with the hydrogels. In our group, native gelatin coating is routinely used to culture these cells. Here, we compared the modified gelatin coatings and found that the cardiomyocytes recovered their spontaneously beating phenotype after overnight culture and continued the beating as long as they were cultured. As the beating was observed, there was no need for Live/Dead staining of the cardiomyocytes.

As no difference was observed between the compositions in the fibroblast culture, we chose to use the highest and lowest ADH-formulations and all CDH-formulations, as listed in Table 1. Phase contrast microscopy showed spreading and migration of the cells from the cardiomyocyte aggregates plated on top of the hydrogel, as seen in Figure 8. The cardiac nature of the differentiated cells was verified by qPCR after 2 weeks in culture and by immunocytochemical staining after 1 week in culture, as shown in Figure 9. The expression of TNNT2 and ACTN2 on the protein level and the expression of these same markers plus MYBPC3 on the RNA level confirms the cardiac nature of our hiPSC-derived cells. The qPCR result in Figure 9a especially shows increased expression of TNNT2 in the 3D hydrogel culture compared to the 2D control, indicating positive cell response. Similarly, Figure 9d shows spreading of TNNT2 positive cells from the cell aggregate into the hydrogel.

The cardiomyocytes were also beating spontaneously under all tested conditions both on top of and encapsulated inside the hydrogels, as can be seen in Videos S6–S10. This

DOI: 10.1021/acsami.8b22343
ACS Appl. Mater. Interfaces 2019, 11, 20589–20602

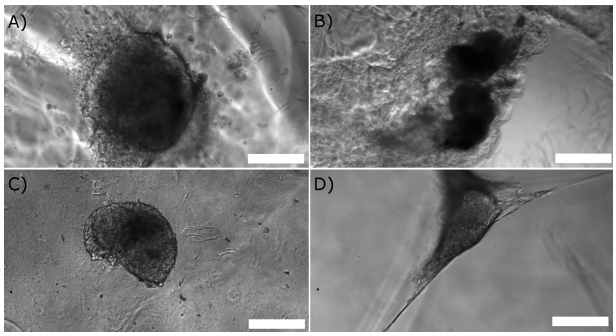

Figure 8. Microscope images of hiPSC-derived cardiomyocyte aggregates cultured under hydrogel conditions: (a) F1-ADH, (b) F3-ADH, (c) F4-CDH, and (d) F5-CDH. The scale bar length is 200 μm.

spontaneous beating is a strong indication of a positive cell response to the culture environment.

The recorded phase contrast videos of cardiomyocyte beating were analyzed with BeatView software that has already been successfully used for hiPSC-derived cardiomyocyte disease modeling in 2D.[11,40] The aggregate beating was not affected by the change of environment from a 2D natural gelatin coated surface to a chemically modified gelatin coating or by being on top of or encapsulated inside the gelatin-GG hydrogel, as shown in Table 2. Cardiomyocytes cultured in the negative control F7-SPD hydrogel did not seem to attach on the hydrogel. They looked worse than in gelatin-GG conditions and did not beat. In the hydrogel culture condition Videos S6–S10, it can be seen how the beating aggregate pulls the hydrogel with it. This observation confirms that suitable elasticity is required of the encapsulating hydrogel, otherwise the cells would be unable to manipulate their surroundings and would be entrapped inside a too rigid hydrogel network; see Videos S6–S11. In the case of two individually beating aggregates in close proximity, this transfer of movement via the hydrogel can be detrimental for the analyzability of the beating. The main beating parameters are shown in Table 2. The beating rate shows how many beats per minute (BPM) are recorded, and the contraction-relaxation duration is the length of a single beat (milliseconds). Between the contractions, the cell is at rest.

The beating behavior observed here is typical for hiPSC-derived cardiomyocytes produced with this differentiation method.[66] The beating frequency remained at ~30 to 70 BPM, regardless of whether the aggregate was cultured on the standard unmodified gelatin coating, on the modified gelatin coating, on top of the hydrogels, or encapsulated inside the hydrogels. Culturing cardiomyocytes in the 3D-engineered heart tissue has been shown to cause their electrophysiology to have a higher resemblance to the real situation in the body.[15] However, the method uses a very weak hydrogel substrate based on Matrigel and relies on the cell's ECM production during the differentiation.[15] Our hydrogel, on the other hand, is strong enough to be handled with tweezers. Subsequently, we can use cells differentiated with any method and move them to hydrogel culture once they start beating, and they recover the beating already after 24 h. The previously discussed Biowire method is a relevant option for cardiomyocyte 3D culture. The method is, however, impeded by the mechanical weakness of Matrigel and greatly constrained by the mold shape.[16] Both of these methods would benefit from replacing the Matrigel-based substrate with our cardiomimetic gelatin-GG hydrogel.

One hurdle to overcome when developing 3D disease modeling is the maturation of hiPSC-derived cardiomyocytes.[67] It has been demonstrated that current differentiation

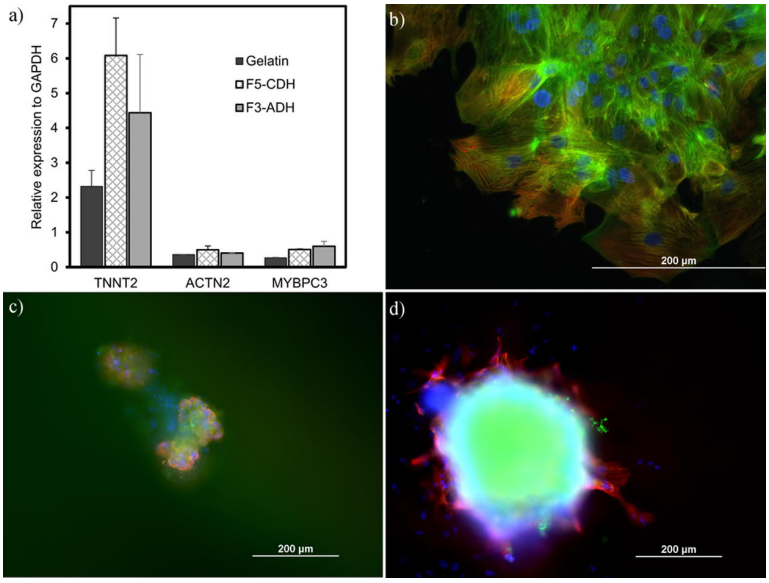

Figure 9. (a) Quantitative RT-PCR validation of cardiac specific genes expressed in hiPSC-derived cardiomyocytes cultured in the gelatin coating control, F5-CDH and F3-ADH. Shown are the expression levels of cardiac type troponin T2 (TNNT2), α-actinin 2 (ACTN2), and Myosin binding protein C (MYBPC3), relative to the housekeeping gene GAPDH. Standard deviations are from three biological replicates, each done in technical triplicate in qPCR. (b–d) Immunocytochemical staining of hiPSC-derived cardiomyocytes using red for TNNT2, green for ACTN2, and blue for DAPI. (b) 2D control on gelatin coating. (c) Aggregate 3D culture in F3-ADH. (d) Aggregate 3D culture in F5-CDH. The density of cell aggregate in F5-CDH slightly prevents antibody and fluorescent light penetration, causing blurriness in the image.

DOI: 10.1021/acsami.8b22343
ACS Appl. Mater. Interfaces 2019, 11, 20589–20602

Table 2. Contraction-Relaxation Durations and Beating Frequencies of the hiPSC-Derived Cardiomyocyte Aggregates Under All Tested Conditions, Analyzed with BeatView Software; $n = 4$

material	2D/3D	ratio[c] [mg mL^{-1}]	beating rate [BPM]	standard deviation	contraction−relaxation duration [ms]	standard deviation
gelatin coating control	2D	100:0	35.78	±20.41	568.60	±127.10[a]
GELA-ADH coating		100:0	42.35	±6.69	435.50	±154.02
GELA-CDH coating		100:0	35.60	±20.18	662.44	±268.50[a]
F7-SPD	3D	0:100	0		0	
F1−3-ADH	2D	40:40	36.71	±17.74	435.25	±113.70
		40:20	68.04	±17.01	305.21	±65.13
	3D	40:40	72.10	±15.14	264.14	±41.97
		40:20	52.70	±47.60	474.59	±303.62[a]
F4−6-CDH	2D	60:60	38.63	[b]	423.74	[b]
		60:40	37.73	±2.78[b]	434.34	±38.96[b]
		40:40	41.56	±5.33	393.14	±63.67
	3D	60:60	35.77	±7.00	403.68	±44.01
		60:40	37.99	±6.50	452.44	±32.85
		40:40	33.82	±3.02	491.88	±15.65

[a]Major prolongation in contraction−relaxation interval detected in one sample. [b]Elasticity of hydrogel transferring movement over a long distance interferes with the beating analysis; so only one or two aggregates were analyzed successfully. [c]Ratio of gelatin to GG.

protocols produce cardiomyocytes that resemble the fetal human heart in gene expression as well as on the structural and functional level.[67,68] There is a multitude of strategies that are aimed at maturing cardiomyocytes. These range from mechanical and electrical stimulations to simply longer culture times.[67] However, the physical cues from the ECM are one potential strategy that we would like to further explore in future. The correct stiffness of the culture substrate as well as its topography can provide cues that can aid the maturation process.[48,67−69] As proven by compression testing (Figure 4), our hydrogels have a biomimicking elasticity that is comparable with the heart tissue. These hydrogels are a promising tool for testing cardiomyocyte maturation. Even though gelatin-ADH-GG hydrogels had a significantly lower strain-hardening effect than gelatin-CDH-GG hydrogels, the beating and mechanotransduction of the cells occur at lower strains and thus make all hydrogel compositions equally promising in this regard.

4. CONCLUSIONS

The current trend in the development of disease models is toward transitioning from 2D cultures to the more biomimicking 3D cultures. This opens up possibilities for studying more tissuelike cellular interactions instead of only studying individual cells. We conclude that the hydrogels based on gelatin-ADH-GG and gelatin-CDH-GG presented in this study are suitable candidates for cardiac TE and 3D cardiac disease modeling. Hydrazide modification of gelatin and oxidation of GG facilitate spontaneous covalent bonding between the polymers. This aids the rapid gelation with homogeneous cross-link distribution under mild conditions suitable for the 3D encapsulation of cells. The stress−strain behavior of hydrogels based on gelatin-CDH very closely resembles the ex vivo heart tissue. The hydrogels enable cell attachment, spreading, and elongation in the encapsulated 3D culture, demonstrated first with human fibroblasts. The hiPSC-derived cardiomyocyte aggregates exhibit normal phenotypical beating behavior when plated on top of or encapsulated inside the hydrogel. On top of the hydrogel, the cardiomyocyte aggregates attached, and cell spreading and migration out of the aggregate were observed. The beating can then be quantitatively analyzed from simple phase contrast microscopy videos with BeatView software, as shown here. The beating analysis shows that cells retain their normal beating characteristics when moved from differentiation in 2D culture to 3D hydrogel culture. No significant biological difference was noticed between the formulations based on gelatin-ADH and gelatin-CDH. Overall, the results suggest the suitability of these gelatin-GG hydrogels with tunable properties for 3D soft tissue modeling and specifically to develop cardiac disease models.

■ ASSOCIATED CONTENT

Supporting Information

The Supporting Information is available free of charge on the ACS Publications website at DOI: 10.1021/acsami.8b22343.

FTIR spectra of GG-CHO compared to unmodified GG; Live/Dead micrographs of fibroblast grown on gelatin-ADH, gelatin-CDH, and unmodified gelatin coatings as well as negative control 3D fibroblast cell culture in F7-SPD composition; and table of the used TaqMan assays for qRT-PCR (PDF)

Reconstruction of bright-field OPT imaging of cultured fibroblasts encapsulated in GELA-ADH-GG 40:20 hydrogel (MPG)

Reconstruction of bright-field OPT imaging of cultured fibroblasts encapsulated in the negative control SPD cross-linked GG hydrogel (MPG)

Beating hiPSC-derived cardiomyocytes on control gelatin coating (AVI)

Beating hiPSC-derived cardiomyocytes on gelatin-ADH coating (AVI)

Beating hiPSC-derived cardiomyocytes on gelatin-CDH coating (AVI)

Beating hiPSC-derived cardiomyocytes in F1-ADH hydrogel culture conditions (AVI)

Beating hiPSC-derived cardiomyocytes in F3-ADH hydrogel culture conditions (AVI)

Beating hiPSC-derived cardiomyocytes in F4-CDH hydrogel culture conditions (AVI)

Beating hiPSC-derived cardiomyocytes in F5-CDH hydrogel culture conditions (AVI)

Beating hiPSC-derived cardiomyocytes in F6-CDH hydrogel culture conditions (AVI)

DOI: 10.1021/acsami.8b22343
ACS Appl. Mater. Interfaces 2019, 11, 20589−20602

Nonbeating hiPSC-derived cardiomyocytes in negative control F7-SPD hydrogel culture conditions (AVI)

AUTHOR INFORMATION

Corresponding Authors

*E-mail: janne.t.koivisto@tuni.fi (J.T.K.).
*E-mail: jenny.parraga@tuni.fi (J.P.).

ORCID

Janne T. Koivisto: 0000-0002-7904-4780
Jari Hyttinen: 0000-0003-1850-3055

Notes

The authors declare no competing financial interest.

ACKNOWLEDGMENTS

The authors would like to thank Alexandre Efimov Ph.D. from the Laboratory of Chemistry and Bioengineering, Faculty of Natural Sciences, Tampere University for his help related to the NMR-measurements, Mari Lehti-Polojärvi M.Sc.(Tech.) from the BioMediTech, Tampere University for the preparation of the custom-made PDMS molds for compression testing samples, Mari Hämäläinen Ph.D. from Immunopharmacology, Tampere University for providing the rabbit heart tissue samples, Eeva Laurila Ph.D. from the BioMediTech, Tampere University for help with BeatView software, and Adj. Prof. Susanna Narkilahti Ph.D., Neuro Group, BioMediTech, Tampere University for help in handling the tissue samples. Additionally, we would like to thank laboratory technicians Henna Lappi and Markus Haponen from the Heart Group, BioMediTech, Tampere University, for providing the differentiated and ready-to-use cardiomyocytes for this study. The authors acknowledge Tampere CellTech Laboratories and Tampere Imaging Facility (TIF) for their services. This work was funded by The Human Spare Parts program of Business Finland (former Tekes—Finnish Funding Agency for Innovation). J.T.K. acknowledges the support given by the Finnish Cultural Foundation Pirkanmaa Regional Fund personal grant number 50151501, and K.A.-S. acknowledges the support by the Finnish Foundation for Cardiovascular Research.

REFERENCES

(1) Langer, R.; Vacanti, J. Tissue Engineering. *Science* **1993**, *260*, 920−926.
(2) Asthana, A.; Kisaalita, W. S. Biophysical Microenvironment and 3D Culture Physiological Relevance. *Drug Discovery Today* **2013**, *18*, 533−540.
(3) Langley, G. R.; Adcock, I. M.; Busquet, F.; Crofton, K. M.; Csernok, E.; Giese, C.; Heinonen, T.; Herrmann, K.; Hofmann-Apitius, M.; Landesmann, B.; Marshall, L. J.; McIvor, E.; Muotri, A. R.; Noor, F.; Schutte, K.; Seidle, T.; van de Stolpe, A.; Van Esch, H.; Willett, C.; Woszczek, G. Towards a 21st-century roadmap for biomedical research and drug discovery: consensus report and recommendations. *Drug Discov. Today* **2017**, *22*, 327−339.
(4) Akopian, V.; Andrews, P. W.; Beil, S.; Benvenisty, N.; Brehm, J.; Christie, M.; Ford, A.; Fox, V.; Gokhale, P. J.; Healy, L.; Holm, F.; Hovatta, O.; Knowles, B. B.; Ludwig, T. E.; McKay, R. D. G.; Miyazaki, T.; Nakatsuji, N.; Oh, S. K. W.; Pera, M. F.; Rossant, J.; Stacey, G. N.; Suemori, H. Comparison of defined culture systems for feeder cell free propagation of human embryonic stem cells. *In Vitro Cell. Dev. Biol.: Anim.* **2010**, *46*, 247−258.
(5) Lu, H. R.; Whittaker, R.; Price, J. H.; Vega, R.; Pfeiffer, E. R.; Cerignoli, F.; Towart, R.; Gallacher, D. J. High Throughput Measurement of Ca++Dynamics in Human Stem Cell-Derived Cardiomyocytes by Kinetic Image Cytometery: A Cardiac Risk Assessment Characterization Using a Large Panel of Cardioactive and Inactive Compounds. *Toxicol. Sci.* **2015**, *148*, 503−516.
(6) Robertson, C.; Tran, D. D.; George, S. C. Concise Review: Maturation Phases of Human Pluripotent Stem Cell-Derived Cardiomyocytes. *Stem Cells* **2013**, *31*, 829−837.
(7) Ojala, M.; Aalto-Setälä, K. Modeling Hypertrophic Cardiomyopathy with Human Induced Pluripotent Stem Cells. In *Pluripotent Stem Cells—from the Bench to the Clinic*; Tomizawa, M., Ed.; InTech: London, U.K., 2016; pp 227−256.
(8) Liang, P.; Lan, F.; Lee, A. S.; Gong, T.; Sanchez-Freire, V.; Wang, Y.; Diecke, S.; Sallam, K.; Knowles, J. W.; Wang, P. J.; Nguyen, P. K.; Bers, D. M.; Robbins, R. C.; Wu, J. C. Drug Screening Using a Library of Human Induced Pluripotent Stem Cell-Derived Cardiomyocytes Reveals Disease-Specific Patterns of Cardiotoxicity. *Circulation* **2013**, *127*, 1677−1691.
(9) Penttinen, K.; Swan, H.; Vanninen, S.; Paavola, J.; Lahtinen, A. M.; Kontula, K.; Aalto-Setälä, K. Correction: Antiarrhythmic Effects of Dantrolene in Patients with Catecholaminergic Polymorphic Ventricular Tachycardia and Replication of the Responses Using iPSC Models. *PLoS One* **2015**, *10*, No. e0134746.
(10) Roden, D. M. Drug-Induced Prolongation of the QT Interval. *N. Engl. J. Med.* **2004**, *350*, 1013−1022.
(11) Ahola, A.; Kiviaho, A. L.; Larsson, K.; Honkanen, M.; Aalto-Setälä, K.; Hyttinen, J. Video Image-Based Analysis of Single Human Induced Pluripotent Stem Cell Derived Cardiomyocyte Beating Dynamics using Digital Image Correlation. *Biomed. Eng. Online* **2014**, *13*, 39−57.
(12) Kuusela, J.; Kujala, V. J.; Kiviaho, A.; Ojala, M.; Swan, H.; Kontula, K.; Aalto-Setälä, K. Effects of Cardioactive Drugs on Human Induced Pluripotent Stem Cell Derived Long QT Syndrome Cardiomyocytes. *Springerplus* **2016**, *5*, 234.
(13) Ribas, J.; Sadeghi, H.; Manbachi, A.; Leijten, J.; Brinegar, K.; Zhang, Y. S.; Ferreira, L.; Khademhosseini, A. Cardiovascular Organ-on-a-Chip Platforms for Drug Discovery and Development. *Appl. In Vitro Toxicol.* **2016**, *2*, 82−96.
(14) Gomes, M. E.; Rodrigues, M. T.; Domingues, R. M. A.; Reis, R. L. Tissue Engineering and Regenerative Medicine: New Trends and Directions-A Year in Review. *Tissue Eng., Part B* **2017**, *23*, 211−224.
(15) Eder, A.; Vollert, I.; Hansen, A.; Eschenhagen, T. Human Engineered Heart Tissue as a Model System for Drug Testing. *Adv. Drug Delivery Rev.* **2016**, *96*, 214−224.
(16) Nunes, S. S.; Miklas, J. W.; Liu, J.; Aschar-Sobbi, R.; Xiao, Y.; Zhang, B.; Jiang, J.; Massé, S.; Gagliardi, M.; Hsieh, A.; Thavandiran, N.; Laflamme, M. A.; Nanthakumar, K.; Gross, G. J.; Backx, P. H.; Keller, G.; Radisic, M. Biowire: a platform for maturation of human pluripotent stem cell-derived cardiomyocytes. *Nat. Methods* **2013**, *10*, 781−787.
(17) Zhu, K.; Shin, S. R.; van Kempen, T.; Li, Y.-C.; Ponraj, V.; Nasajpour, A.; Mandla, S.; Hu, N.; Liu, X.; Leijten, J.; Lin, Y.-D.; Hussain, M. A.; Zhang, Y. S.; Tamayol, A.; Khademhosseini, A. Gold Nanocomposite Bioink for Printing 3D Cardiac Constructs. *Adv. Funct. Mater.* **2017**, *27*, 1605352.
(18) Zhang, Y. S.; Arneri, A.; Bersini, S.; Shin, S.-R.; Zhu, K.; Goli-Malekabadi, Z.; Aleman, J.; Colosi, C.; Busignani, F.; Dell'Erba, V.; Bishop, C.; Shupe, T.; Demarchi, D.; Moretti, M.; Rasponi, M.; Dokmeci, M. R.; Atala, A.; Khademhosseini, A. Bioprinting 3D Microfibrous Scaffolds for Engineering Endothelialized Myocardium and Heart-on-a-Chip. *Biomaterials* **2016**, *110*, 45−59.
(19) Walters, N. J.; Gentleman, E. Evolving insights in cell-matrix interactions: Elucidating how non-soluble properties of the extracellular niche direct stem cell fate. *Acta Biomater.* **2015**, *11*, 3−16.
(20) Nakamura, K.; Shinoda, E.; Tokita, M. The Influence of Compression Velocity on Strength and Structure for Gellan Gels. *Food Hydrocoll.* **2001**, *15*, 247−252.
(21) Koivisto, J. T.; Joki, T.; Parraga, J. E.; Pääkkönen, R.; Ylä-Outinen, L.; Salonen, L.; Jönkkäri, I.; Peltola, M.; Ihalainen, T. O.; Narkilahti, S.; Kellomäki, M. Bioamine-Crosslinked Gellan Gum Hydrogel for Neural Tissue Engineering. *Biomed. Mater.* **2017**, *12*, 025014.

DOI: 10.1021/acsami.8b22343
ACS Appl. Mater. Interfaces 2019, 11, 20589−20602

(22) Karvinen, J.; Koivisto, J. T.; Jönkkäri, I.; Kellomäki, M. The Production of Injectable Hydrazone Crosslinked Gellan Gum-Hyaluronan-Hydrogels with Tunable Mechanical and Physical Properties. *J. Mech. Behav. Biomed. Mater.* **2017**, *71*, 383−391.
(23) Koivusalo, L.; Karvinen, J.; Sorsa, E.; Jönkkäri, I.; Väliaho, J.; Kallio, P.; Ilmarinen, T.; Miettinen, S.; Skottman, H.; Kellomäki, M. Hydrazone Crosslinked Hyaluronan-Based Hydrogels for Therapeutic Delivery of Adipose Stem Cells to Treat Corneal Defects. *Mater. Sci. Eng., C* **2018**, *85*, 68−78.
(24) Karvinen, J.; Joki, T.; Ylä-Outinen, L.; Koivisto, J. T.; Narkilahti, S.; Kellomäki, M. Soft Hydrazone Crosslinked Hyaluronan- and Alginate-Based Hydrogels as 3D Supportive Matrices for Human Pluripotent Stem Cell-Derived Neuronal Cells. *React. Funct. Polym.* **2018**, *124*, 29−39.
(25) Dubruel, P.; Unger, R.; Van Vlierberghe, S.; Cnudde, V.; Jacobs, P. J. S.; Schacht, E.; Kirkpatrick, C. J. Porous Gelatin Hydrogels: 2. In Vitro Cell Interaction Study. *Biomacromolecules* **2007**, *8*, 338−344.
(26) Van Den Bulcke, A. I.; Bogdanov, B.; De Rooze, N.; Schacht, E. H.; Cornelissen, M.; Berghmans, H. Structural and Rheological Properties of Methacrylamide Modified Gelatin Hydrogels. *Biomacromolecules* **2000**, *1*, 31−38.
(27) Bacelar, A. H.; Silva-Correia, J.; Oliveira, J. M.; Reis, R. L. Recent progress in gellan gum hydrogels provided by functionalization strategies. *J. Mater. Chem. B* **2016**, *4*, 6164−6174.
(28) Ferris, C. J.; Stevens, L. R.; Gilmore, K. J.; Mume, E.; Greguric, I.; Kirchmajer, D. M.; Wallace, G. G.; in het Panhuis, M. Peptide Modification of Purified Gellan Gum. *J. Mater. Chem. B* **2015**, *3*, 1106−1115.
(29) da Silva, L. P.; Jha, A. K.; Correlo, V. M.; Marques, A. P.; Reis, R. L.; Healy, K. E. Gellan Gum Hydrogels with Enzyme-Sensitive Biodegradation and Endothelial Cell Biorecognition Sites. *Adv. Healthcare Mater.* **2018**, *7*, 1700686.
(30) Silva-Correia, J.; Gloria, A.; Oliveira, M. B.; Mano, J. F.; Oliveira, J. M.; Ambrosio, L.; Reis, R. L. Rheological and Mechanical Properties of Acellular and Cell-Laden Methacrylated Gellan Gum Hydrogels. *J. Biomed. Mater. Res., Part A* **2013**, *101*, 3438−3446.
(31) Yue, K.; Trujillo-de Santiago, G.; Alvarez, M. M.; Tamayol, A.; Annabi, N.; Khademhosseini, A. Synthesis, Properties, and Biomedical Applications of Gelatin Methacryloyl (GelMA) Hydrogels. *Biomaterials* **2015**, *73*, 254−271.
(32) Shin, H.; Olsen, B. D.; Khademhosseini, A. The Mechanical Properties and Cytotoxicity of Cell-Laden Double-Network Hydrogels Based on Photocrosslinkable Gelatin and Gellan Gum Biomacromolecules. *Biomaterials* **2012**, *33*, 3143−3152.
(33) Fedorovich, N. E.; Oudshoorn, M. H.; van Geemen, D.; Hennink, W. E.; Alblas, J.; Dhert, W. J. A. The Effect of Photopolymerization on Stem Cells Embedded in Hydrogels. *Biomaterials* **2009**, *30*, 344−353.
(34) Williams, C. G.; Malik, A. N.; Kim, T. K.; Manson, P. N.; Elisseeff, J. H. Variable Cytocompatibility of Six Cell Lines with Photoinitiators used for Polymerizing Hydrogels and Cell Encapsulation. *Biomaterials* **2005**, *26*, 1211−1218.
(35) Mironi-Harpaz, I.; Wang, D. Y.; Venkatraman, S.; Seliktar, D. Photopolymerization of Cell-Encapsulating Hydrogels: Crosslinking Efficiency Versus Cytotoxicity. *Acta Biomater.* **2012**, *8*, 1838−1848.
(36) Figueiras, E.; Soto, A. M.; Jesus, D.; Lehti, M.; Koivisto, J.; Parraga, J. E.; Silva-Correia, J.; Oliveira, J. M.; Reis, R. L.; Kellomäki, M.; Hyttinen, J. Optical Projection Tomography as a Tool for 3D Imaging of Hydrogels. *Biomed. Opt. Express* **2014**, *5*, 3443−3449.
(37) Coutinho, D. F.; Sant, S. V.; Shin, H.; Oliveira, J. T.; Gomes, M. E.; Neves, N. M.; Khademhosseini, A.; Reis, R. L. Modified Gellan Gum Hydrogels with Tunable Physical and Mechanical Properties. *Biomaterials* **2010**, *31*, 7494−7502.
(38) Schneider, C. A.; Rasband, W. S.; Eliceiri, K. W. NIH Image to ImageJ: 25 Years of Image Analysis. *Nat. Methods* **2012**, *9*, 671−675.
(39) Belay, B.; Koivisto, J. T.; Vuornos, K.; Montonen, T.; Koskela, O.; Lehti-Polojärvi, M.; Miettinen, S.; Kellomäki, M.; Figueiras, E.; Hyttinen, J. Optical Projection Tomography Imaging of Single Cells in 3D Gellan Gum Hydrogel. In *EMBEC & NBC 2017: Joint Conference of the European Medical and Biological Engineering Conference (EMBEC) and the Nordic-Baltic Conference on Biomedical Engineering and Medical Physics (NBC), Tampere, Finland, June 2017*; Eskola, H., Väisänen, O., Viik, J., Hyttinen, J., Eds.; Springer Singapore: Singapore, 2018; pp 996−999.
(40) Kiviaho, A. L.; Ahola, A.; Larsson, K.; Penttinen, K.; Swan, H.; Pekkanen-Mattila, M.; Venäläinen, H.; Paavola, K.; Hyttinen, J.; Aalto-Setälä, K. Distinct Electrophysiological and Mechanical Beating Phenotypes of Long QT Syndrome Type 1-Specific Cardiomyocytes Carrying Different Mutations. *Int. J. Cardiol. Heart Vasc.* **2015**, *8*, 19−31.
(41) Lian, X.; Zhang, J.; Azarin, S. M.; Zhu, K.; Hazeltine, L. B.; Bao, X.; Hsiao, C.; Kamp, T. J.; Palecek, S. P. Directed cardiomyocyte differentiation from human pluripotent stem cells by modulating Wnt/β-catenin signaling under fully defined conditions. *Nat. Protoc.* **2012**, *8*, 162−175.
(42) Laurila, E.; Ahola, A.; Hyttinen, J.; Aalto-Setälä, K. Methods for in vitro functional analysis of iPSC derived cardiomyocytes - Special focus on analyzing the mechanical beating behavior. *Biochim. Biophys. Acta, Mol. Cell Res.* **2016**, *1863*, 1864−1872.
(43) Livak, K. J.; Schmittgen, T. D. Analysis of Relative Gene Expression Data Using Real-Time Quantitative PCR and the 2−ΔΔCT Method. *Methods* **2001**, *25*, 402−408.
(44) Prestwich, G. D.; Marecak, D. M.; Marecek, J. F.; Vercruysse, K. P.; Ziebell, M. R. Controlled Chemical Modification of Hyaluronic Acid: Synthesis, Applications, and Biodegradation of Hydrazide Derivatives. *J. Controlled Release* **1998**, *53*, 93−103.
(45) Vandooren, J.; Van den Steen, P. E.; Opdenakker, G. Biochemistry and Molecular Biology of Gelatinase B Or Matrix Metalloproteinase-9 (MMP-9): The Next Decade. *Crit. Rev. Biochem. Mol. Biol.* **2013**, *48*, 222−272.
(46) Shim, J. L. N. J.. U.S. Patent 4,517,216. Gellan gum/gelatin blends, 1985.
(47) Kozlov, P. V.; Burdygina, G. I. The Structure and Properties of Solid Gelatin and the Principles of their Modification. *Polymer* **1983**, *24*, 651−666.
(48) Amano, Y.; Nishiguchi, A.; Matsusaki, M.; Iseoka, H.; Miyagawa, S.; Sawa, Y.; Seo, M.; Yamaguchi, T.; Akashi, M. Development of Vascularized iPSC Derived 3D-Cardiomyocyte Tissues by Filtration Layer-by-Layer Technique and their Application for Pharmaceutical Assays. *Acta Biomater.* **2016**, *33*, 110−121.
(49) Mathur, A.; Loskill, P.; Shao, K.; Huebsch, N.; Hong, S.; Marcus, S. G.; Marks, N.; Mandegar, M.; Conklin, B. R.; Lee, L. P.; Healy, K. E. Human iPSC-Based Cardiac Microphysiological System for Drug Screening Applications. *Sci. Rep.* **2015**, *5*, 8883.
(50) Oliveira, M. B.; Custódio, C. A.; Gasperini, L.; Reis, R. L.; Mano, J. F. Autonomous Osteogenic Differentiation of hASCs Encapsulated in Methacrylated Gellan-Gum Hydrogels. *Acta Biomater.* **2016**, *41*, 119−132.
(51) Koshy, S. T.; Desai, R. M.; Joly, P.; Li, J.; Bagrodia, R. K.; Lewin, S. A.; Joshi, N. S.; Mooney, D. J. Click-Crosslinked Injectable Gelatin Hydrogels. *Adv. Healthcare Mater.* **2016**, *5*, 541−547.
(52) Zhao, X.; Lang, Q.; Yildirimer, L.; Lin, Z. Y.; Cui, W.; Annabi, N.; Ng, K. W.; Dokmeci, M. R.; Ghaemmaghami, A. M.; Khademhosseini, A. Photocrosslinkable Gelatin Hydrogel for Epidermal Tissue Engineering. *Adv. Healthcare Mater.* **2016**, *5*, 108−118.
(53) Mirsky, I.; Parmley, W. W. Assessment of Passive Elastic Stiffness for Isolated Heart Muscle and the Intact Heart. *Circ. Res.* **1973**, *33*, 233−243.
(54) Levental, I.; Georges, P. C.; Janmey, P. A. Soft Biological Materials and their Impact on Cell Function. *Soft Matter* **2007**, *3*, 299−306.
(55) Neal, R. A.; Jean, A.; Park, H.; Wu, P. B.; Hsiao, J.; Engelmayr, G. C., Jr.; Langer, R.; Freed, L. E. Three-Dimensional Elastomeric Scaffolds Designed with Cardiac-Mimetic Structural and Mechanical Features. *Tissue Eng., Part A* **2013**, *19*, 793−807.

DOI: 10.1021/acsami.8b22343
ACS Appl. Mater. Interfaces 2019, 11, 20589−20602

(56) Oyen, M. L. Mechanical Characterisation of Hydrogel Materials. *Int. Mater. Rev.* **2014**, *59*, 44−59.
(57) Bashir, B.; Iyer, R. K.; Chen Wen, L. K.; Ruogang, Z.; Sider, K. L.; Morakot, L.; Simmons, C. A.; Milica, R. Influence of Substrate Stiffness on the Phenotype of Heart Cells. *Biotechnol. Bioeng.* **2010**, *105*, 1148−1160.
(58) Engler, A. J.; Carag-Krieger, C.; Johnson, C. P.; Raab, M.; Tang, H.-Y.; Speicher, D. W.; Sanger, J. W.; Sanger, J. M.; Discher, D. E. Embryonic Cardiomyocytes Beat Best on a Matrix with Heart-Like Elasticity: Scar-Like Rigidity Inhibits Beating. *J. Cell Sci.* **2008**, *121*, 3794−3802.
(59) Melchels, F. P. W.; Dhert, W. J. A.; Hutmacher, D. W.; Malda, J. Development and Characterisation of a New Bioink for Additive Tissue Manufacturing. *J. Mater. Chem. B* **2014**, *2*, 2282−2289.
(60) Nichol, J. W.; Koshy, S. T.; Bae, H.; Hwang, C. M.; Yamanlar, S.; Khademhosseini, A. Cell-Laden Microengineered Gelatin Methacrylate Hydrogels. *Biomaterials* **2010**, *31*, 5536−5544.
(61) Wen, C.; Lu, L.; Li, X. An Interpenetrating Network Biohydrogel of Gelatin and Gellan Gum by using a Combination of Enzymatic and Ionic Crosslinking Approaches. *Polym. Int.* **2014**, *63*, 1643−1649.
(62) *SFS-EN ISO 10993-5 Biological Evaluation of Medical Devices. Part 5: Tests for in Vitro Cytotoxicity*; Finnish Standards Association: Helsinki, Finland, 2009.
(63) Appel, A. A.; Anastasio, M. A.; Larson, J. C.; Brey, E. M. Imaging Challenges in Biomaterials and Tissue Engineering. *Biomaterials* **2013**, *34*, 6615−6630.
(64) Hayflick, L.; Moorhead, P. S. The Serial Cultivation of Human Diploid Cell Strains. *Exp. Cell Res.* **1961**, *25*, 585−621.
(65) Wang, C.; Gong, Y.; Lin, Y.; Shen, J.; Wang, D.-A. A Novel Gellan Gel-Based Microcarrier for Anchorage-Dependent Cell Delivery. *Acta Biomater.* **2008**, *4*, 1226−1234.
(66) Vuorenpää, H.; Penttinen, K.; Heinonen, T.; Pekkanen-Mattila, M.; Sarkanen, J.-R.; Ylikomi, T.; Aalto-Setälä, K. Maturation of Human Pluripotent Stem Cell Derived Cardiomyocytes is Improved in Cardiovascular Construct. *Cytotechnology* **2017**, *69*, 785−800.
(67) Tan, S. H.; Ye, L. Maturation of Pluripotent Stem Cell-Derived Cardiomyocytes: a Critical Step for Drug Development and Cell Therapy. *J Cardiovasc Transl Res* **2018**, *11*, 375−392.
(68) Tzatzalos, E.; Abilez, O. J.; Shukla, P.; Wu, J. C. Engineered Heart Tissues and Induced Pluripotent Stem Cells: Macro- and Microstructures for Disease Modeling, Drug Screening, and Translational Studies. *Adv. Drug Delivery Rev.* **2016**, *96*, 234−244.
(69) Besser, R. R.; Ishahak, M.; Mayo, V.; Carbonero, D.; Claure, I.; Agarwal, A. Engineered Microenvironments for Maturation of Stem Cell Derived Cardiac Myocytes. *Theranostics* **2018**, *8*, 124−140.

DOI: 10.1021/acsami.8b22343
ACS Appl. Mater. Interfaces 2019, 11, 20589−20602